Synthesis of Monodisperse Chitosan Nanoparticles and in Situ Drug Loading Using Active Microreactor

Vivek Kamat, Ila Marathe, Vandana Ghormade,* Dhananjay Bodas,* and Kishore Paknikar*

Nanobioscience, Agharkar Research Institute, GG Agarkar Road, Pune 411 004, India

Ⓢ Supporting Information

ABSTRACT: Chitosan nanoparticles are promising drug delivery vehicles. However, the conventional method of unregulated mixing during ionic gelation limits their application because of heterogeneity in size and physicochemical properties. Therefore, a detailed theoretical analysis of conventional and active microreactor models was simulated. This led to design and fabrication of a polydimethylsiloxane microreactor with magnetic micro needles for the synthesis of monodisperse chitosan nanoparticles. Chitosan nanoparticles synthesized conventionally, using 0.5 mg/mL chitosan, were 250 ± 27 nm with +29.8 ± 8 mV charge. Using similar parameters, the microreactor yielded small size particles (154 ± 20 nm) at optimized flow rate of 400 μL/min. Further optimization at 0.4 mg/mL chitosan concentration yielded particles (130 ± 9 nm) with higher charge (+39.8 ± 5 mV). The well-controlled microreactor-based mixing generated highly monodisperse particles with tunable properties including antifungal drug entrapment (80%), release rate, and effective activity (MIC, 1 μg/mL) against *Candida*.

KEYWORDS: *chitosan nanoparticles, active microreactor, microneedle, drug loading, antifungal activity*
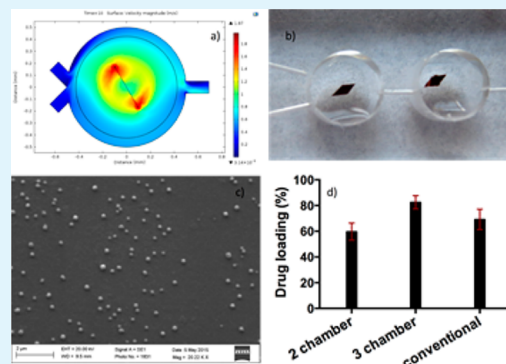
1. INTRODUCTION

Chitosan nanoparticles have attracted attention as drug delivery vehicles due to their ability to protect the drug from degradation, increase loading and release it in a slow sustained manner.[1,2] These nanoparticles are synthesized from chitosan, a natural polymer containing acetylated and deacetylated glucosamine units, that displays biocompatibility and biodegradability and is generally recognized as safe.[3,4] Chitosan nanoparticles (CNPs) have shown promising results in drug delivery for treatment of diabetes and cancer.[5−8] The main challenge in the application of chitosan nanoparticles is faced during their controlled size synthesis, a character that significantly affects their use as drug delivery vehicles.

Synthesis of these particles by microemulsion, reverse micellar, and coacervation techniques utilize either organic solvents or harmful cross-linkers that could be toxic.[1,9] In comparison, the ionic gelation method based on the electrostatic interaction between amine groups of chitosan and negatively charged phosphate group of sodium tripolyphosphate (TPP) utilize mild conditions suitable for drug delivery.[10−12] Typically, synthesis of chitosan nanoparticles by ionic gelation involves the dropwise addition of the cross-linker (TPP) to the polymer (chitosan) solution by slow, uncontrolled bulk mixing. This method, though eco-friendly and safe, yields nanoparticles with variable sizes (250−400 nm) and charge (+25 to +54 mV).[13−16] This heterogeneity in size further affects their physicochemical characters such as charge, loading efficiency and controlled drug release.[11,17−19] Moreover, variation in parameters such as reactant concentration,

selection of cross-linker and molecular weight of chitosan failed to yield homogeneous particles.[11,18,20] Other approaches employing ultrasonication and radiation amplitude were investigated for their role in decreasing the size and polydispersity without much effect.[21] Recently, "microfluidic drifting" a methodology of 3D fluid manipulation in a single monolith layer, has been introduced.[22−26] The optimal operational parameters were predicted by mathematical modeling and geometric design of the inlet holes and channels of the device. The designs were fine-tuned for the flow of the polymer and the cross-linker in to a reaction chamber and subsequent collection of the synthesized nanoparticles at the outlet.

Microfluidic synthesis offers the controlled movement of reactants and their interaction in a precise volume to yield monodisperse nanoparticles. Usually, researchers employ a passive route of synthesis of nanoparticle using microfluidics, where scaling effects confine the fluid dynamics to a laminar regime with characteristic low Reynolds number (*Re*). Passive mixing faces drawbacks in terms of slow rate and low efficiency of mixing.[27] Hence, active micromixers that disturb the laminar flow to realize mixing have great potential.[28] Active mechanisms increase the interfacial area between two fluids by complex flow pattern and facilitate mixing primarily by chaotic advection and by diffusion. Active microreactors demonstrate faster mixing in
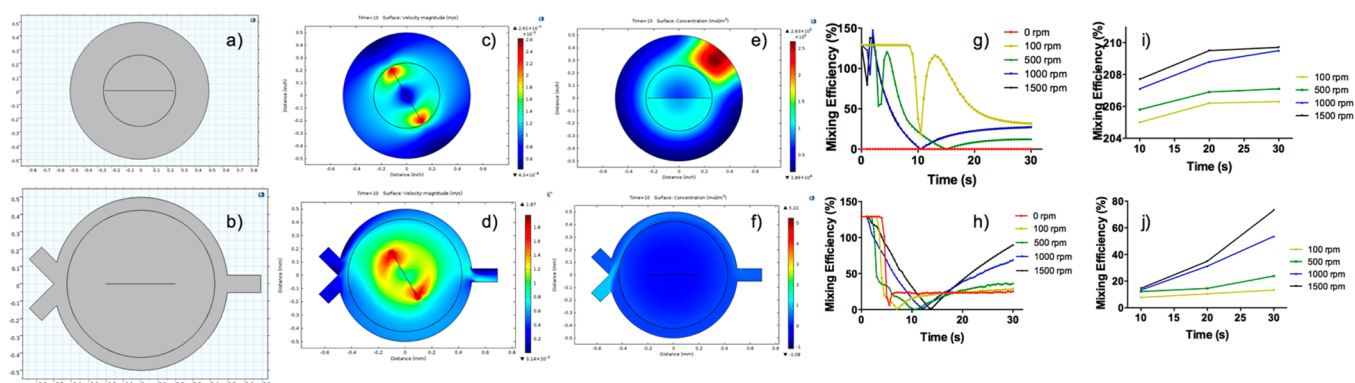
Figure 1. 2D simulation of conventional and microreactor using Comsol multiphysics 4.4. (a, b) Schematic of 2D models used for simulating conventional and active microreactor. (c, d) Velocity profile; (e, f) concentration of the mixed liquid obtained; (g, h) mixing efficiency calculated from the simulation and (i, j) experimentally derived mixing efficiency for conventional and microreactor.

small volumes with more control. Not many research papers have demonstrated synthesis of chitosan nanoparticles using active microreactors. One reason might be difficulty of the fabrication process; the other might be tuning/harnessing the energies associated with the active reaction for controlled synthesis. Yang et al.[29] have used cross-flow microfluidic chip with external cross-linking for synthesis of monodisperse chitosan microparticles. With flow focusing and emulsion technique, microbeads of chitosan were obtained. Majedi et al.[22,30,31] have used T-shaped microreactor for synthesis of monodisperse chitosan nanoparticles via self-assembly. The size of the obtained nanoparticles was around 100 nm using nanogelation with adenosine triphosphate (ATP) as a cross-linker. Anticancer drug (paclitaxel) was loaded on these nanoparticles and its efficacy was demonstrated. The authors have demonstrated high loading efficiency with slow and sustained release.

In the current work, we first carried out modeling for the synthesis of chitosan nanoparticles using conventional and active microreactors with an aim to understand the advantages of the latter leading to small, homogeneous particles. This knowledge was translated by fabricating a microreactor in PDMS containing magnetic microneedles for the active synthesis of chitosan nanoparticles. The fabrication simplicity of this method was further exploited for loading CNPs with amphotericin B (AmB), an antifungal drug. Here we demonstrate microreactor synthesized chitosan nanoparticles were monodisperse and showed improved size, charge, and drug loading as compared to bulk synthesized nanoparticles. We report the effectiveness of drug-loaded CNPs as an antifungal agent against *Candida* and its hemocompatibility.

2. THEORETICAL ANALYSIS

Understanding the dynamics of conventional and micromixing was important for fabrication of a microreactor for the synthesis of CNPs by ionic gelation. Therefore, classical and microreactor setup using single reaction chamber were modeled and analyzed using Comsol Multiphysics 4.4.

Conventional- and microreactor simulation models in 2D geometry are shown in Figure 1a, b. For a conventional model, a liquid bath ($\phi 25$ mm) containing chitosan solution is considered with a submerged magnetic needle (length 1 cm) for mixing. While mixing, the needle rests at the bottom of the vessel, which creates a vortex and practically no mixing occurs

at the center. Therefore, TPP droplets were added away from the center while modeling.

The microreactor model consists of two separate inlets (ϕ 0.5 mm) to allow the flow of chitosan and TPP leading to a circular chamber ($\phi 1$ mm) containing the magnetic actuator (length 0.5 mm). The circular chamber has single outlet (ϕ 0.5 mm). The magnetic needle induced maximum confluence of fluids entering from inlets due to stirring. At the microscale, diffusion is a dominant mechanism whereby two different fluids come together and mix. The microreactor model assumes steady state, laminar, and incompressible flow, governed by continuity, Navier–Stokes, and species transport by convection–diffusion. Simulations were carried out with variation in rotation speed as well as time and the results are analyzed with respect to mixing efficiency calculated using the formula given below[32]

$$ M = \sqrt{ \frac{ \frac{1}{N} \sum_{i=1}^{N} \left(\overline{c} - c_i/\overline{c} \right)^2 }{ \overline{c}_0 \left(1 - \overline{c}_0 \right)^2 } } $$

where c is the concentration and N is the reaction number. Prefix i and 0 indicate final and initial concentrations, respectively.

Figure 1c, d shows the velocity profiles (indicative) obtained from 2D simulation of conventional and active microreactor models. As compared to the conventional model, microreactor achieves better mixing due large force generated with greater velocity, at similar operating parameters. The concentration profile (Figure 1e, f), shows uniform mixing of the liquid in microreactor as compared to an unmixed gradient observed in the conventional model, at the same time interval. Figure 1g, h shows an increase in mixing efficiency with rpm. In the first few seconds, the mixing efficiency drops drastically for both conventional and microreactor before attaining saturation. As the rotor applies confluence, the liquid is taken to different parts of the chamber decreasing the mixing efficiency in the initial stage. The efficiency obtained for microreactor is much higher as compared to the conventional technique, with a maximum of ~90% in 30 s. These models were validated experimentally by using blue and yellow colored liquids. The mixed liquid was collected from the outlet at different time points from the microreactor and was withdrawn with a pipet from the conventional setup. The droplets were placed on a paraffin wax film, and photographs were captured using a digital camera (Cannon). The images were analyzed by ImageJ
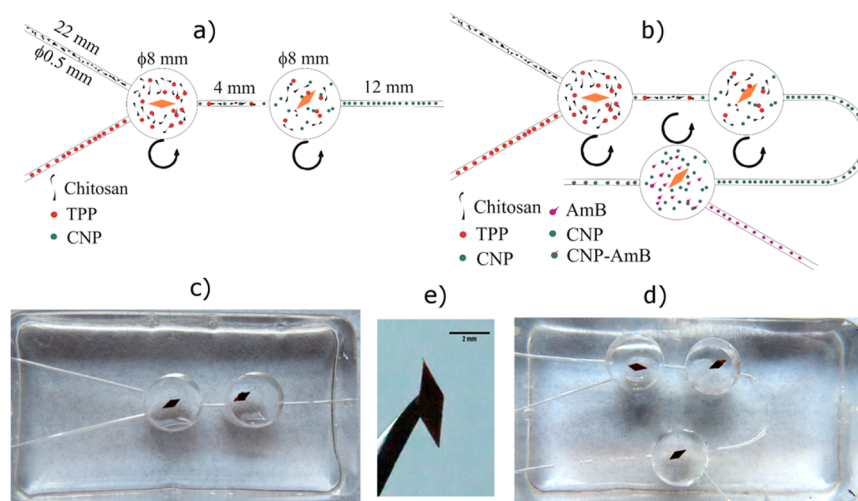
Figure 2. Schematic representation and optical image of fabricated microreactor chip for (a, c) chitosan nanoparticles synthesis by 2-chamber method, (b, d) drug loading by 3-chamber method; (e) rhombic magnetic needle.

software for green intensity. Readings were normalized using a premixed green color as control, and mixing efficiency was calculated in percentage. It can be seen from Figure 1i, j that mixing efficiency of the microreactor is greater than that of the conventional at same time points. Moreover, mixing efficiency increases as a function of time and rotational speed complying with the result of the simulation studies. The maximum efficiency obtained from microreactor is ~80% that is in good agreement with simulation data (~90%).

There is a distinct difference between mixing by the conventional and microreactor setup. One reactant is added dropwise to another (liquid bath) at different time points conventionally whereas the continuous fluid flow is obtained by mixing in a microreactor. Equilibrium is reached faster in conventional setup resulting in a drop in the diffusion coefficient and Reynolds number leading to laminar flow like condition, which restricts further mixing. On the other hand, because of continuous flow in the microreactor and flow out through the outlets, fresh volumes of two fluids enter the chamber and mix, leading to higher mixing efficiency.

From the theoretical analysis, it is important to note that the increment in efficiency is significant in the first few seconds of stirring (Figure 1g, h), saturating exponentially as time increases. This observation implies that the microreactor achieves efficient mixing within a few seconds of contact of the two liquids. It is evident that the rise in rpm above 1000 did not have a significant impact on the mixing efficiency. Hence, all the further experiments were carried out at the rotational speed of 1000 rpm. With a single reactor, the mixing efficiency of ~80% was achieved. To enhance the efficiency and to promote synthesis of nanoparticles with uniform size, we added another reaction chamber (Figure 2a, c). A third stage of the reaction chamber and an inlet channel (Figure 2b, d) was added for loading the drug on synthesized chitosan nanoparticles. The magnetic needle was fabricated in a rhombic shape (Figure 2e) to have maximum confluence while mixing in a microreactor.

3. MATERIALS AND METHODS

3.1. Chip and Micro Magnetic Needle Fabrication. Microreactor with circular channels and chamber was fabricated from poly(dimethylsiloxane) (PDMS)[33] using soft lithography (Supplementary). The chip was fabricated with 2 inlet channels, (ϕ 500 μm)

which permit the reactants to flow into the first chamber (ϕ 8 mm) containing a micro needle (see Figure 2a, c). The mixed fluids are carried through a 4 mm long channel to the second chamber similar to the first, for further mixing. Both the chambers were sealed using a thin glass cover. PDMS-magnetic needle (Figure 2e) was fabricated[34] as detailed in the Supporting Information (page S-1).

For drug loading, a third chamber (ϕ 8 mm) was fabricated connected to the second by a 22 mm long channel. A 10 mm long inlet was added to the third well, to introduce the drug for entrapment in polymeric nanoparticles (see Figure 2 b, d).

3.2. Synthesis of Chitosan Nanoparticles: Conventional and Microreactor Method. Chitosan nanoparticles were synthesized by ionic gelation using chitosan (Sigma, deacetylation: 75−85%; viscosity: > 400 mPa.s) dissolved in 1% acetic acid (pH 3.3) and sodium tripolyphosphate (TPP, Merck, 1.6 mg/mL) in the ratio of 2.5:1 (Calvo et al. 1997). TPP (0.625, 1.25, and 1.87 mL) was added dropwise with a micropipette to 5 mL of 0.25, 0.5, and 0.75 mg/mL chitosan solution, respectively, under magnetic stirring (1000 rpm) at room temperature (For schematic, refer to Figure S1). Whereas, chitosan and TPP in similar ratio were allowed to flow (flow rate: 100−500 μL/min) in the microreactor for the synthesis of monodisperse nanoparticles. (Detailed description of the methodology is added in Supporting Information on page S-1).

3.3. Characterization Techniques. Number or particles/ml along with the size was determined using Nanosight LM10, UK.Zeta potential was measured using Delsa Nano from Beckman Coulter, USA. The morphology of chitosan nanoparticles was recorded using an FEI Technai 30 system, Oregon, USA operated at 300 kV. Atomic force microscopy (AFM) measurements were performed with Multiview 1000 System, Nanonics Imaging Ltd., Israel. Scanning electron microscopy (SEM) was carried out using Zeiss EVO MA 15 instrument using tungsten filament as a source. FTIR measurements were performed on PerkinElmer (Spectrum One Spectrometer).

3.4. Drug Loading and Release Kinetics. Drug entrapment was carried out at CNP:AmB ratio of 1:1with 0.2 mg each CNPs and drug (dissolved in DMSO). On-chip drug loading was accomplished by two different methods and chip designs, viz. (a) introduction of drug along with TPP through one inlet (using a 2 inlet chip) while chitosan through the other and (b) introduction of drug through a third inlet (of a 3 inlet chip) after the synthesis of CNPs. The AmB entrapment efficiency (A.E.) of nanoparticles was calculated by recording the absorbance of unbound AmB at 420 nm using the formula

$$\text{drug entrapment (\%)} = \frac{\text{total AmB} - \text{free AmB}}{\text{total AmB}} 100$$

3.5. In Vitro Release of Drug. Amphotericin B release was determined spectrophotometrically at different time points (up to 14
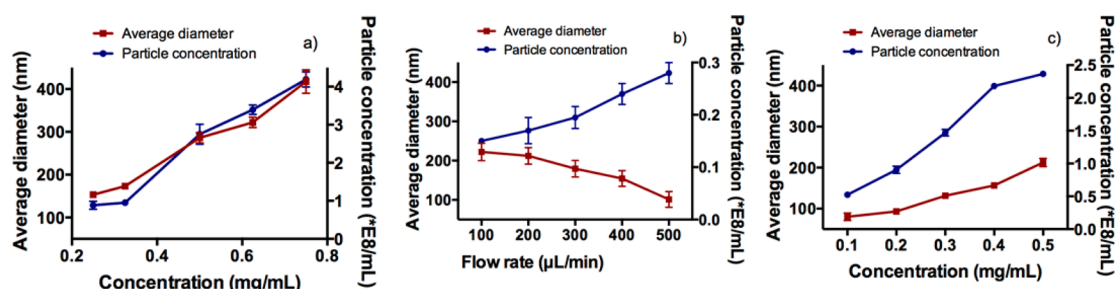
Figure 3. Chitosan nanoparticles synthesis by (a) conventional method and optimization of microreactor based on-chip method by (b) altering the flow rate, (c) altering the chitosan concentrations at constant flow rate.

days) by incubating the loaded CNP in 1 mL of phosphate buffer (pH 7.0 at 37 °C).

3.6. Size-Dependent Nanoparticle Internalization/Uptake in Cells. For cell internalization experiments, MCF-7 cells were grown in 6-well plates with 0.5 × 0.5 cm cover glass for 24 h. Fluorescein isothiocyanate (FITC); a green fluorescent moiety was loaded in the CNPs during synthesis for microscopic visualization. The FITC–CNPs synthesized by microreactor and conventional method were then added to the cells at a concentration of 30 μg/ml and incubated for 4 h. Three washes with PBS were given to the cells to remove any nanoparticles adhering nonspecifically to the cell surfaces. The cells were stained with DAPI for nuclear and phalloidin-TRITC for the cytoskeleton staining, respectively. Mounting media (90% glycerol in 0.8% Tris-Cl buffer pH 7.0 containing ascorbic acid) was added to the cells and observations were carried out with a confocal microscope (LSM 710, Carl Zeiss, Jena, Germany with Zen 2009 software for image analysis) equipped with appropriate filters.

3.7. Antifungal Assay. The antifungal assay was carried out with *Candida albicans* (NCIM 3100) acquired from National Collection of Industrial Microorganisms, National Chemical Laboratory, Pune, India. Antifungal assay was carried out using NCCLS guidelines M27 (Supporting Information on page S-2).

3.8. Hemo-compatibility. Hemolysis studies were conducted by the procedures described by the American Society for Testing and Materials (ASTM F756−00, 2000). Detailed methodology is given in the Supporting Information (pages S-2 and S-3).

4. RESULTS AND DISCUSSION

4.1. Conventional Method. CNPs were synthesized by the conventional method using a fixed chitosan to TPP ratio of 2.5:1 but varying chitosan (0.25 to 0.75 mg/mL) and TPP (0.625 to 1.87 mg/mL) concentrations and the size of the synthesized particles was measured. In general, an increase in the concentration of the reactants led to an increase in particle size (149 ± 19 to 462 ± 37 nm) and number of particles/mL (0.81- 4.33E8) (Figure 3a). At chitosan concentration of 0.5 mg/mL, the size of CNPs was 302 ± 27 nm with 2.98E8 particle/mL and +29.8 ± 8 mV zeta potential.

The results obtained are as predicted by theoretical analysis where the increase in concentration leads to a decrease in the diffusion coefficient and Reynolds number to yield large size NPs. The inherent difficulties encountered regarding particle size and homogeneity with the conventional method was addressed by employing the microreactor approach.

It needs to be mentioned that chitosan nanoparticles synthesis by bulk methods have used chitosan and TPP ratios of 3:1, 4:1, and 5:1, where ∼200 nm sized NPs have been reported.[11,13,14] Most significantly, at a ratio of 2.5:1, that has been used in the present study, previously reported CNP size is much higher, i.e., 321 nm.[18]

4.2. Microreactor Method. In the microreactor, microchannels were used to carry chitosan and TPP simultaneously into the chamber where mixing was initiated. Microfluidic properties such as flow rate and the reactant ratio determined the quality of synthesized CNPs. TPP and chitosan were mixed in the chamber to form nanoparticles that flowed through the outlet, therefore reducing the chances of clogging. Conditions for CNPs synthesis was similar to that used conventionally.

To translate the process to the micromixer platform, at constant chitosan concentration of 0.5 mg/mL, we optimized the flow rate from 100 to 500 μL/min (Figure 3b). As the flow rate increased, the particle size decreased with 1.8 fold reduction in standard deviation (Figure 3b). At a flow rate of 500 μL/min, the channel at the outlet ruptured because of the high pressure. Hence, a flow rate of 400 μL/min was optimized where the channels sustained the pressure and yielded 154 ± 20 nm sized CNPs with 0.24E8 particles/mL (Figure 3b).

Further, to increase the number of particles, the reactant concentration was varied (0.1−0.5 mg/mL) at optimized flow rate 400 μL/min (Figure 3c). Because the specific flow rate maintained, concentration and diffusion coefficient of the total reaction volume was constant, resulting in homogeneous particle size. At lower reactant concentration (0.1 mg/mL), smaller NPs (80 ± 9 nm) with lower number of particles (0.52 E8particles/ml), whereas at higher reactant concentrations (0.5 mg/mL), a higher number of particles (2.36E8 particles/mL) with larger size (212 ± 10 nm) were formed. At chitosan and TPP concentrations of 0.4 and 0.16 mg/mL, respectively, the obtained particle size was to the tune of 130 ± 9 nm. The number of particles in the preparation was 2.1×10^8/mL with a zeta potential of 39.8 ± 5 mV (Figure 3c). In the conventional synthesis, significantly larger (more than 50%) particles with lower zeta potential were obtained. The standard deviation is also very less with microreactor method implying homogeneity in particle synthesis.

Therefore, CNPs synthesized with 400 μL/min flow rate and 0.4 mg/mL chitosan concentration were used for drug loading and assessment of antifungal activity against *Candida*. The same protocol could be extended for the batch synthesis of drug loaded chitosan nanoparticles with good homogeneity in particle size (Details are given in Figure S2).

4.3. Comparison of Conventional and Microreactor-Based Synthesis of Chitosan Nanoparticles. Zeta potential determination of chitosan nanoparticles synthesized conventionally exhibited a charge of +29 ± 6 mV, whereas that by microreactor method were higher +40 ± 8 mV. This result implied an increase in the colloidal stability of the particles.

Atomic force and transmission electron microscopic analysis confirmed the sizes for bulk and microreactor synthesized CNPs as ∼250 and ∼130 nm, respectively (Figure 4). CNPs synthesized by microreactor were smooth (confirmed by RMS value of <0.1 from AFM), spherical and homogeneous in size,
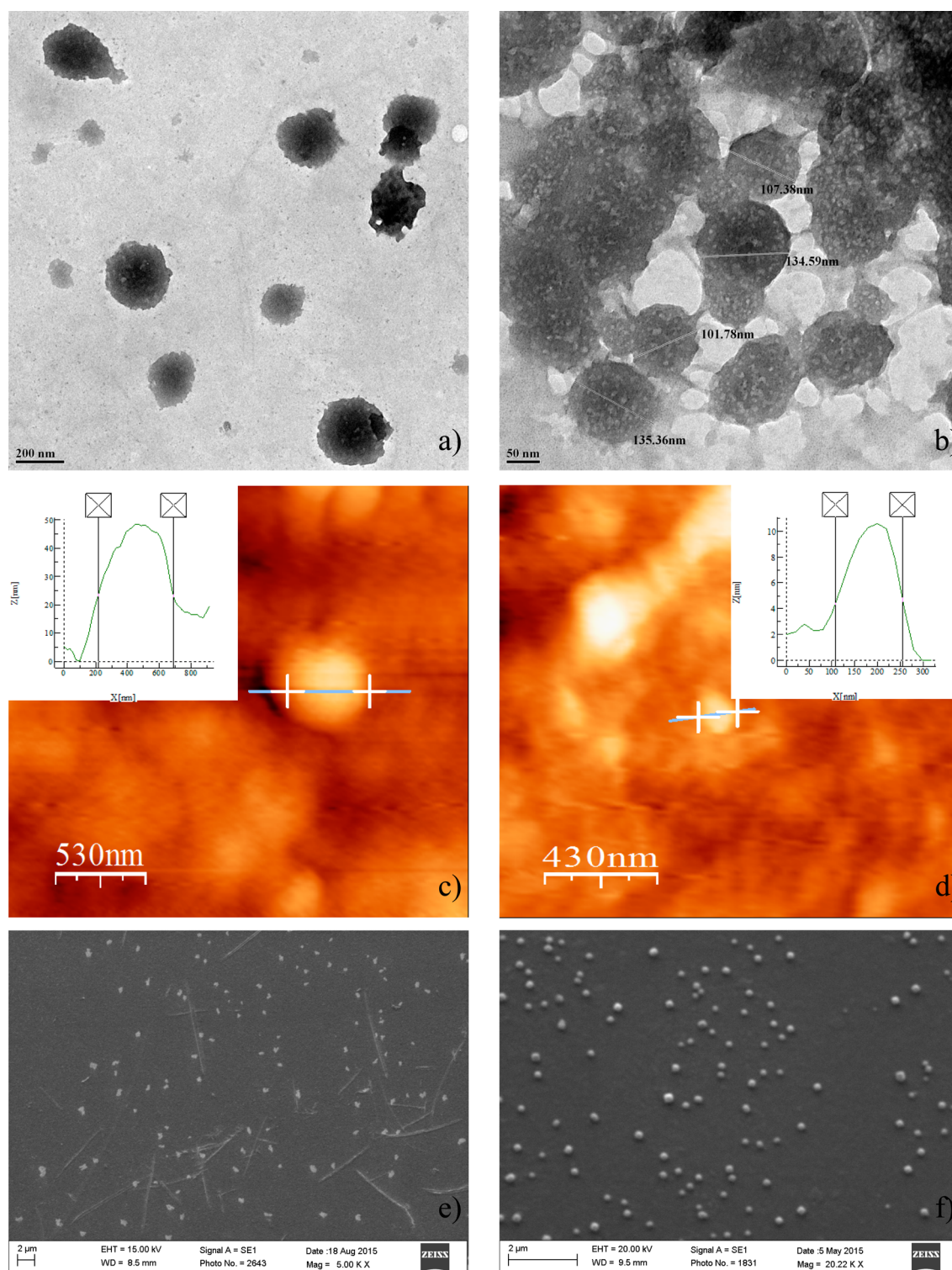
Figure 4. Characterization of chitosan nanoparticles: (a, b) transmission electron microscopy; (c, d) atomic force microscopy (inset shows size estimation curve from atomic force micrograph) and(e, f) scanning electron microscopy for conventional and microreactor method, respectively.

whereas conventional synthesis produced heterogeneous particles of spherical to ovoid shape. TEM reveals blurred walls due to incomplete reaction for nanoparticles synthesized conventionally. Significant reduction in size and increment in homogeneity is obtained by microreactor with an improvement in morphology. The SEM images show high degree of monodispersivity along with smaller size for nanoparticles

synthesized using microreactor method as compared to those obtained conventionally.

4.4. Entrapment of Amphotericin B by on-Chip Synthesized Chitosan Nanoparticles. Two approaches were used for on-chip loading of amphotericin B (AmB) as represented in the schematic (Figure 2). In the first approach, drug and TPP were allowed to flow via one channel and chitosan through the other in a 2-chamber chip (Figure 2c).

Concurrently, nanoparticles were synthesized along with drug entrapment in the first chamber followed by enhanced mixing in the second. Drug entrapment obtained with the 2-chamber chip was 59.7%. (Figure 5a).
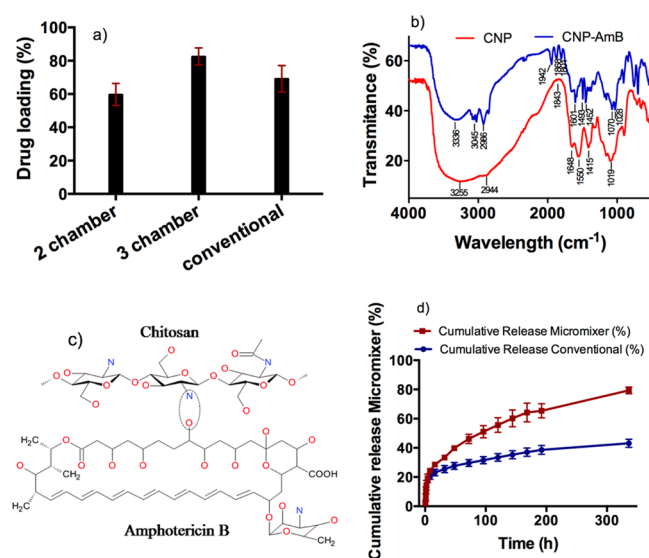

Figure 5. Drug entrapment and release from chitosan nanoparticles: (a) amphotericin entrapment by on-chip two-way channel and three-way channel method as compared to conventional method, (b) FTIR analysis of chitosan nanoparticles and entrapment of amphotericin, (c) probable binding of amphotericin to chitosan, (d) release of amphotericin from chitosan nanoparticles.

In the second approach, an additional chamber was added to introduce and load the drug on synthesized chitosan nanoparticles (Figure 2d). The drug entrapment achieved with this approach was 82.7% that was much higher than the two chamber method. In comparison to the conventional method with 70% drug entrapment, the microreactor synthesis showed an increase in drug entrapment (Figure 5a). This significant increase in drug loading by microreactor method could be due to the measured interaction of the CNP and drug in the microreactor chamber. This phenomenon coupled with monodisperse size distribution enhances the drug loading efficiency due to increment in surface to volume ratio as reported by Majedi et al.[22] An alteration in charge of the AmB-loaded CNPs (+34.41 mV), and size (188 nm) was observed as compared to bare that may be attributed to the presence of the drug.

Most studies report drug entrapment by the bulk method.[35,36] Tiyaboonchai and Limpeanchob[37] demonstrate 50−65% AmB drug entrapment with chitosan-dextran nanoparticles. Nahar et al.[38] reported 49% entrapment of AmB in gelatin nanoparticles cross-linked with glutaraldehyde.

4.5. Fourier Transform Infrared Spectroscopy (FTIR) Analysis of CNP-AmB. Fourier transform infrared (FTIR) spectra of the CNPs and CNP-AmB are shown in Figure 5b. Amphotericin is an amphoteric drug having hydrophobic and hydrophilic moieties whereas chitosan is known to possess amine groups on the glucosamine moiety. The proposed attachment could involve the − OH and − NH$_2$ groups of amphotericin and chitosan respectively (Figure 5c). The characteristic absorption bands for chitosan were observed at 1648 (amide I), 1550 (amide II), 1453 (amide III), 1099(C−N stretching), and 3255 cm^{-1} (O−H stretching).[39] The characteristic absorption bands for the AmB were reported at 2986 cm^{-1} for the polyene group (CH$_2$, CH$_3$, and CH) and 1692 cm^{-1} for the COO$^-$ group.[40] The spectrum for CNP-AmB showed the appearance of absorption bands of carboxyl groups at 1801, 1868, 1942 cm^{-1} that may be attributed to the adherence of amphotericin to chitosan, amide group of chitosan at 1452 and 1493 cm^{-1} with an additional peak at 1601 cm^{-1} (Figure 5b). The absorption peaks at 3336, 3045, and 2986 cm^{-1} could be assigned to the OH groups of CNP-AmB. The shift of existing and presence of additional peak could be attributed to the presence of amphotericin indicating the entrapment of AmB within the chitosan matrix.

4.6. In Vitro Drug Release of AmB from Chitosan Nanoparticles. Figure 5d displays the biphasic release profile of AmB from microreactor synthesized CNPs at pH 7.0. It was apparent that initial burst release was followed by the slow sustained release of ∼52% in 120 h and 80% in 336 h. The rapid release was attributed to the surface bound drug followed by slow release due to drug diffusion from the interior of chitosan nanoparticles. The in vitro release behavior suggests that the interaction forces between amphotericin and chitosan were weak indicating AmB release by simple dissociation. In the case of conventionally synthesized CNPs, although AmB showed a biphasic release, the drug release was ∼33% in 120 h and 43% in 336 h. The rapid release in the case of nanoparticles synthesized using microreactor can be attributed to smaller size, which possess higher surface to volume ratio as compared to the conventional counterparts.[41] This clearly
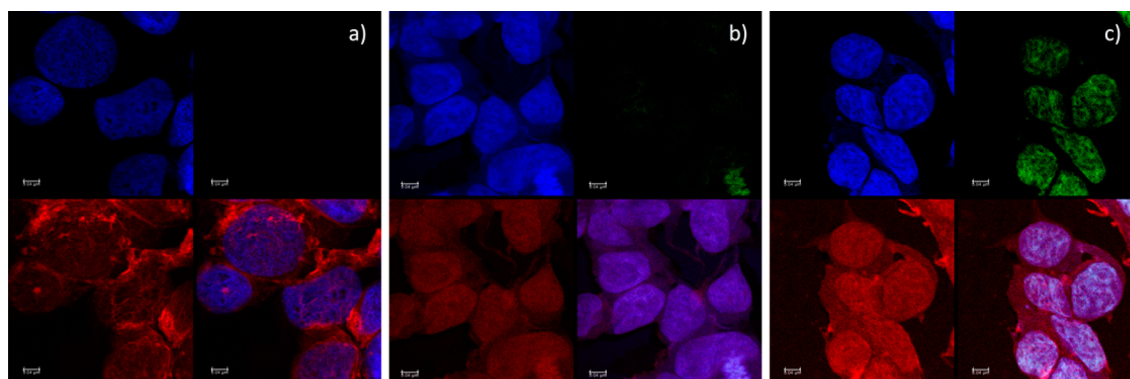

Figure 6. Confocal imaging of MCF-7 cells (a) control (without nanoparticles) and uptake of nanoparticles synthesized by (b) conventional method and (c) microreactor method.
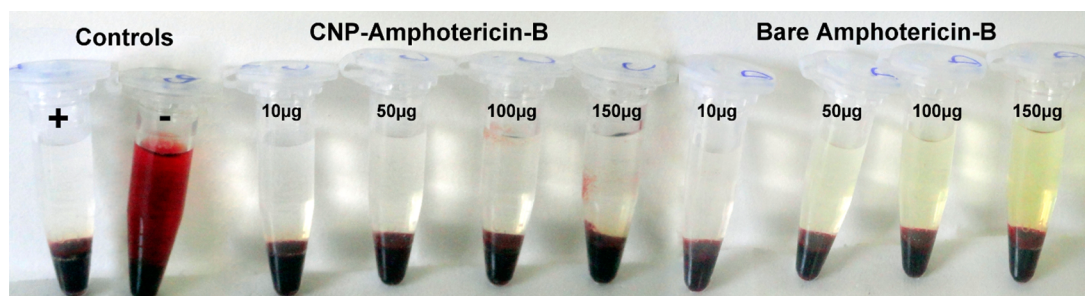
Figure 7. Hemolytic activity of chitosan nanoparticles-amphotericin, bare amphotericin, and positive and negative control.

demonstrated the effect of particle size on drug release. Nahar et al.[38] reported 90% biphasic drug release of AmB from gelatin nanoparticles up to 196 h. However, Tiyaboonchai and Limpeanchob[37] reported that chitosan-dextran sulfate nanoparticles showed a rapid release. Espeulas et al.[42] observed that *Candida* was more sensitive to polymeric nanoparticle-bound AmB than the free drug.

4.7. Size-Dependent Nanoparticle Internalization/ Uptake in Cells. The uptake of chitosan nanoparticles in MCF-7 cell lines was visualized (after 4 h of exposure) by confocal microscopy, for the two synthesis methods (Figure 6). Control cells (Figure 6a), which are not exposed to nanoparticles, show blue nuclear staining with DAPI and red (Phalloidin TRITC) cytoskeleton staining. The chitosan nanoparticles were modified by FITC and visualized by green fluorescence under the microscope. The uptake of chitosan nanoparticles (~250 nm) synthesized by conventional method was negligible (Figure 6b). The ~130 nm sized microreactor synthesized nanoparticles were localized within the cell as seen by the green fluorescence (Figure 6c). This clearly demonstrated the size-dependent property of chitosan nanoparticles during the uptake in the MCF-7 cells.

4.8. In Vitro Antifungal Activity of CNP-AmB against *Candida*. The on-chip drug entrapment of AmB in CNPs displayed effective antifungal activity against *Candida*. The CNP-AmB displayed minimum inhibitory concentration (MIC) value of 1 μg/mL which is accordance with that for bare amphotericin B.[43,44] The MIC for the CNPs prepared by conventional method was comparable that could be attributed to the similar release profile at 24 h time point used for the antifungal assay. Majedi et al.[31] also reported rapid release in the initial (<24 h) phase for different sized particles. The MIC value was also comparable to the commercially available lipid preparation (refer to Figure S3). The results demonstrate that the drug loaded CNPs were effective against *Candida*. Similar results with AmB loaded PLGA nanoparticles were reported by Zhou et al.[44]

AFM analysis of *Candida* cells treated with bare AmB showed that the surface roughness (RMS 0.53) was comparable to cells treated with CNP-AmB (RMS 0.5). A further analysis of roughness by skewness and kurtosis values showed that chitosan-AmB treatment disrupts the cell wall in comparison to bare drug attributed to the synergistic effect of chitosan and drug (refer to Figures S4 and S5 and Table S1).

4.9. Hemo-Compatibility. The assay was performed according to the Standard Practice for Assessment of Hemolytic properties of Materials from the American Society for Testing and Materials (ASTM F756−00, 2000), which classifies the material as nonhemolytic (0−2% of hemolysis), slightly hemolytic (2−5% of hemolysis) and hemolytic (>5% of

hemolysis). Our results (Figure 7) showed that bare AmB (3% hemolysis) and CNP-AmB (2.6% hemolysis) were non-hemolytic up to concentrations of 0.16 mM.

5. CONCLUSION

The simulation studies carried out showed better mixing in the case or microreactor as fresh reagents come in contact due to flow rate dependency, which is not the case in the conventional setup. The initial time (in ms) for the formation of particles is significant, as seen from the theoretical analysis. As the microreactor is operated at high flow rate, synthesized nanoparticles flow out, decreasing the hold time of the reactants in the chamber, leading to lower size and homogeneity of preparation. The microreactor yields nanoparticles of size 130 ± 9 nm with 39.8 ± 5 mV surface charge, whereas 250 ± 27 nm size and 29.8 ± 8 mV charge was obtained by conventional method. The microreactor by virtue of its measured volume interactions allowed high drug (amphotericin) entrapment that displayed a slow sustained release. In vitro, CNP-AmB yielded effective fungicidal effect against *Candida albicans*, demonstrating good hemo-compatibility. The microreactor can also be used in a batch mode for the synthesis of a large amount of homogeneous particles without variation in size and charge.

■ ASSOCIATED CONTENT

ⓢ Supporting Information

The Supporting Information is available free of charge on the ACS Publications website at DOI: 10.1021/acsami.5b05100.

> Methodology for conventional synthesis. Batch synthesis using microreactor for scale up; effect of bare drug and loaded drug-nanoparticle complex on *Candida* using Live−Dead staining and AFM (PDF)

■ AUTHOR INFORMATION

Corresponding Authors
*E-mail: vandanaghormade@aripune.org. Tel: +912025325000.
*E-mail: dsbodas@aripune.org.
*E-mail: kpaknikar@gmail.com

Author Contributions
V.G. and D.B. planned and designed experiments and cowrote the paper. K.M.P. provided intellectual inputs. D.B. carried out the theoretical analysis and helped in characterization and analysis of results. I.M. carried out conventional method. V.K. fabricated the chip and carried out synthesis using microreactor method.

Notes
The authors declare no competing financial interest.

■ REFERENCES

(1) Patel, J. K.; Jivani, N. P. Chitosan Based Nanoparticles In Drug Delivery. *Int. J. Pharm. Sci. Nanotechnol.* **2009**, *2*, 517−522.

(2) Soppimath, K. S.; Aminabhavi, T. M.; Kulkarni, A. R.; Rudzinski, W. E. Biodegradable Polymeric Nanoparticles As Drug Delivery Devices. *J. Controlled Release* **2001**, *70*, 1−20.

(3) Wang, J. J.; Zeng, Z. W.; Xiao, R. Z.; Xie, T.; Zhou, G. L.; Zhan, X. R.; Wang, S. L. Recent Advances Of Chitosan Nanoparticles As Drug Carriers. *Int. J. Nanomed.* **2011**, *6*, 765−774.

(4) Keawchaoon, L.; Yoksan, R. Preparation, Characterization And In Vitro Release Study Of Carvacrol-Loaded Chitosan Nanoparticles Colloids Surf B. *Colloids Surf., B* **2011**, *84*, 163−171.

(5) Pan, Y.; Li, Y. J.; Zhao, H. Y.; Zheng, J. M.; Xu, H.; Wei, G.; Hao, J. S.; Cui, F. D. Bioadhesive Polysaccharide In Protein Delivery System: Chitosan Nanoparticles Improve The Intestinal Absorption Of Insulin *In Vivo*. *Int. J. Pharm.* **2002**, *249*, 139−147.

(6) Sung, H. W.; Sonaje, K.; Liao, Z. X.; Hsu, L. W.; Chuang, E. Y. pH-Responsive Nanoparticles Shelled With Chitosan For Oral Delivery Of Insulin: From Mechanism To Therapeutic Applications. *Acc. Chem. Res.* **2012**, *45*, 619−629.

(7) Arulmozhi, V.; Pandian, S.; Mirunalini. Ellagic Acid Encapsulated Chitosan Nanoparticles For Drug Delivery System In Human Oral Cancer Cell Line (KB) Colloids Surf B. *Colloids Surf., B* **2013**, *110*, 313−320.

(8) Goethals, E. C.; Elbaz, A.; Lopata, A. L.; Bhargava, S. K.; Bansal, V. Decoupling The Effects Of The Size, Wall Thickness, And Porosity Of Curcumin-Loaded Chitosan Nanocapsules On Their Anticancer Efficacy: Size Is The Winner. *Langmuir* **2013**, *29*, 658−666.

(9) Tokumitsu, H.; Ichikawa, H.; Fukumori, Y. Chitosan−Gadopentetic Acid Complex Nanoparticles For Gadolinium Neutron Capture Therapy Of Cancer: Preparation By Novel Emulsion-Droplet Coalescence Technique And Characterization. *Pharm. Res.* **1999**, *16*, 1830−1835.

(10) Calvo, P.; Remunan-Lopez, C.; Vila-Jato, J. L.; Alonso, M. J. Novel Hydrophilic Chitosan−Polyethylene Oxide Nanoparticles As Protein Carriers. *J. Appl. Polym. Sci.* **1997**, *63*, 125−132.

(11) Gan, Q.; Wang, T.; Cochrane, C.; McCarron, P. Modulation Of Surface Charge, Particle Size And Morphological Properties Of Chitosan−Tpp Nanoparticles Intended For Gene Delivery Colloids Surf. B. *Colloids Surf., B* **2005**, *44*, 65−73.

(12) Shu, X. Z.; Zhu, K. J. A Novel Approach To Prepare Tripolyphosphate/Chitosan Complex Beads For Controlled Release Drug Delivery. *Int. J. Pharm.* **2000**, *201*, 51−58.

(13) Fernandez-Urrusuno, R.; Calvo, P.; Remunan-Lopez, C.; Vila-Jato, J. L.; Alonso, M. J. Enhancement Of Nasal Absorption Of Insulin Using Chitosan Nanoparticles. *Pharm. Res.* **1999**, *16*, 1576−1581.

(14) Gan, Q.; Wang, T. Chitosan Nanoparticle As Protein Delivery Carrier-Systematic Examination Of Fabrication Conditions For Efficient Loading And Release Colloids Surf.B. *Colloids Surf., B* **2007**, *59*, 24−34.

(15) Koukaras, E. N.; Papadimitriou, S. A.; Bikiaris, D. N.; Froudakis, G. E. Insight On The Formation Of Chitosan Nanoparticles Through Ionotropic Gelation With Tripolyphosphate. *Mol. Pharmaceutics* **2012**, *9*, 2856−2862.

(16) Ghormade, V.; Gholap, H.; Kale, S.; Kulkarni, V.; Bhat, S.; Paknikar, K. Fluorescent Cadmium Telluride Quantum Dots Embedded Chitosan Nanoparticles: A Stable, Biocompatible Preparation For Bio-Imaging. *J. Biomater. Sci., Polym. Ed.* **2015**, *26*, 42−56.

(17) Grenha, A.; Seijo, B.; Remunan-Lopez, C. Microencapsulated Chitosan Nanoparticles For Lung Protein Delivery. *Eur. J. Pharm. Sci.* **2005**, *25*, 427−437.

(18) Liu, H.; Gao, C. Preparation And Properties Of Ionically Cross-Linked Chitosan Nanoparticles. *Polym. Adv. Technol.* **2009**, *20*, 613−619.

(19) Mattu, C.; Li, R.; Ciardelli, G. Chitosan Nanoparticles As Therapeutic Protein Nanocarriers: The Effect Of pH On Particle Formation And Encapsulation Efficiency. *Polym. Compos.* **2013**, *34*, 1538−1545.

(20) Jonassen, H.; Kjoeniksen, A. L.; Hiorth, M. Stability Of Chitosan Nanoparticles Cross-Linked With Tripolyphosphate. *Biomacromolecules* **2012**, *13*, 3747−3756.

(21) Tang, E. S. K.; Huang, M.; Lim, L. Y. Ultrasonication Of Chitosan And Chitosan Nanoparticles. *Int. J. Pharm.* **2003**, *265*, 103−114.

(22) Majedi, F. S.; Hasani-Sadrabadi, M. M.; VanDersarl, J. J.; Mokarram, N.; Hojjati-Emami, S.; Dashtimoghadam, E.; Bonakdar, S.; Shokrgozar, M. A.; Bertsch, A.; Renaud, P. On-Chip Fabrication Of Paclitaxel-Loaded Chitosan Nanoparticles For Cancer Therapeutics. *Adv. Funct. Mater.* **2014**, *24*, 432−441.

(23) Valencia, P.; Pridgen, E. M.; Rhee, M.; Langer, R.; Faroukhzad, O. C.; Karnik, R. Microfluidic Platform For Combinatorial Synthesis And Optimization Of Targeted Nanoparticles For Cancer Therapy. *ACS Nano* **2013**, *7*, 10671−10680.

(24) Shen, H.; Hong, S.; Prudhomme, R. K.; Liu, Y. Self Assembling Process Of Flash Nano Precipitation In A Multi-Inlet Vortex Mixer To Produce Drug Loaded Polymeric Nanoparticles. *J. Nanopart. Res.* **2011**, *13*, 4109−4120.

(25) Xu, Q.; Hashimoto, M.; Dang, T. T.; Hoare, T.; Kohane, D. S.; Whitesides, G. M.; Langer, R.; Erson, D. G. Preparation Of Monodisperse Biodegradable Polymer Microparticles Using A Microfluidic Flow-Focusing Device For Controlled Drug Delivery. *Small* **2009**, *13*, 1575−1581.

(26) Karnik, R.; Gu, F.; Basto, P.; Cannizzaro, C.; Dean, L.; Kyei-Manu, W.; Langer, R.; Faroukhzad, O. C. Microfluidic Platform For Controlled Synthesis Of Polymeric Nanoparticles. *Nano Lett.* **2008**, *8*, 2906−2912.

(27) Rhee, M.; Valencia, P. M.; Rodriguez, M. I.; Langer, R.; Faroukhzad, O. C.; Karnik, R. Synthesis Of Size-Tunable Polymeric Nanoparticles Enabled By 3d Hydrodynamic Flow Focusing In Single-Layer Microchannels. *Adv. Mater.* **2011**, *23*, 79−83.

(28) Hung, L. S.; Lee, A. P. Microfluidic Devices For The Synthesis Of Nanoparticles And Biomaterials. *J. Medical Biol. Eng.* **2007**, *27*, 1−6.

(29) Yang, C.; Huang, K.; Lin, P.; Lin, Y. Using A Cross-Flow Microfluidic Chip And External Crosslinking Reaction For Monodisperse TPP-Chitosan Microparticles. *Sens. Actuators, B* **2007**, *124*, 510−516.

(30) Majedi, F. S.; Hasani-Sadrabadi, M. M.; Mokarram, N.; Hojjati-Emami, S.; Taghipoor, M.; Dashtimoghadam, E.; Bertsch, A.; Moaddel, H.; Renaud, P. Microfluidic Synthesis Of Chitosan-Based Nanoparticles For Fuel Cell Applications. *Chem. Commun.* **2012**, *48*, 7744−7746.

(31) Majedi, F. S.; Hasani-Sadrabadi, M. M.; Hojjati-Emami, S.; Shokrgozar, M. A.; VanDersarl, J. J.; Dashtimoghadam, E.; Bertsch, A.; Renaud, P. Microfludic Assisted Self-Assembly Of Chitosan Based Nanoparticles As Drug Delivery Agents. *Lab Chip* **2013**, *13*, 204−207.

(32) Veldurthi, N.; Chandel, S.; Bhave, T. M.; Bodas, D. Computational Fluid Dynamic Analysis Of Poly(Dimethyl Siloxane) Magnetic Actuator Based Micromixer. *Sens. Actuators, B* **2015**, *212*, 419−424.

(33) Agrawal, S.; Morarka, M.; Bodas, D.; Paknikar, K. M. Multiplexed detection of water borne pathogens using circular microfluidics. *Appl. Biochem. Biotechnol.* **2012**, *167*, 1668−1677.

(34) Bute, M.; Sheikh, A.; Mathe, V.; Bodas, D.; Karekar, R.; Gosawi, S. Magnetically Controlled Flexible Valve For Flow Manipulation In Polymer Microfluidic Devices. *Proc. IEEE* **2012**, 357−360.

(35) Papadimitriou, S.; Bikiaris, D.; Avgoustakis, K.; Karavas, E.; Georgarakis, M. Chitosan Nanoparticles Loaded With Dorzolamide And Pramipexole. *Carbohydr. Polym.* **2008**, *73*, 44−54.

(36) Vandervoort, J.; Ludwig, A. Preparation And Evaluation Of Drug-Loaded Gelatin Nanoparticles For Topical Ophthalmic Use. *Eur. J. Pharm. Biopharm.* **2004**, *57*, 251−261.

(37) Tiyaboonchai, W.; Limpeanchob, N. Formulation And Characterization Of Amphotericin B−Chitosan−Dextran Sulfate Nanoparticles. *Int. J. Pharm.* **2007**, *329*, 142−149.

(38) Nahar, M.; Mishra, D.; Dubey, V.; Jain, N. K. Development, Characterization, And Toxicity Evaluation Of Amphotericin B−Loaded Gelatin Nanoparticles Nanomed. *Nanomedicine* **2008**, *4*, 252−261.

(39) Van de Velde, K.; Kiekens, P. Structure Analysis And Degree Of Substitution Of Chitin, Chitosan And Dibutyrylchitin By FTIR Spectroscopy And Solid State ^{13}C NMR. *Carbohydr. Polym.* **2004**, *58*, 409−416.

(40) Gagoś, M.; Arczewska, M. Spectroscopic Studies Of Molecular Organization Of Antibiotic Amphotericin B In Monolayers And Dipalmitoylphosphatidylcholine Lipid Multibilayers. *Biochim. Biophys. Acta, Biomembr.* **2010**, *1798*, 2124−2130.

(41) Fan, Y.; Li, C.; Cao, H.; Li, F.; Chen, D. The Intranuclear Release Of A Potential Anticancer Drug From Small Nanoparticles That Are Derived From Intracellular Dissociation Of Large Nanoparticles. *Biomaterials* **2012**, *33*, 4220−4228.

(42) Espuelas, M. S.; Legrand, P.; Campanero, M. A.; Appel, M.; Chéron, M.; Gamazo, C.; Barratt, G.; Irache, J. M. Polymeric Carriers For Amphotericin B: In Vitro Activity, Toxicity And Therapeutic Efficacy Against Systemic Candidiasis In Neutropenic Mice. *J. Antimicrob. Chemother.* **2003**, *52*, 419−427.

(43) Arendrup, M.; Lundgren, B.; Jensen, I. M.; Hansen, B. S.; Fridmodt M?ller, N. Comparison Of E Test And A Tablet Diffusion Test With Nccls Broth Microdilution Method For Flucanozole And Amphotericin B Susceptibility Testing Of *Candida*. *J. Antimicrob. Chemother.* **2001**, *47*, 521−526.

(44) Zhou, W.; Wang, Y.; Jian, J.; Song, S. Self-Aggregated Nanoparticles Based On Amphiphilicpoly(Lactic Acid)-Grafted-Chitosan Copolymer For Ocular Delivery Of Amphotericin B. *Int. J. Nanomed.* **2013**, *8*, 3715−3728.